

---

# Identifying Co-Adaptation of Algorithmic and Implementational Innovations in Deep Reinforcement Learning: A Taxonomy and Case Study of Inference-based Algorithms

---

Hiroki Furuta<sup>1</sup> Tadashi Kozuno<sup>2</sup> Tatsuya Matsushima<sup>1</sup> Yutaka Matsuo<sup>1</sup> Shixiang Shane Gu<sup>3</sup>

## Abstract

Recently many algorithms were devised for reinforcement learning (RL) with function approximation. While they have clear algorithmic distinctions, they also have many implementation differences that are algorithm-agnostic and sometimes subtle. Such mixing of algorithmic novelty and implementation craftsmanship makes rigorous analyses of the sources of performance improvements difficult. In this work, we focus on a series of inference-based actor-critic algorithms – MPO, AWR, and SAC – to decouple their algorithmic innovations and implementation decisions. We present unified derivations through a single control-as-inference objective, where we can categorize each algorithm as based on either Expectation-Maximization (EM) or direct Kullback–Leibler (KL) divergence minimization and treat the rest of specifications as implementation details. We performed extensive ablation studies, and identified substantial performance drops whenever implementation details are *mismatched* for algorithmic choices. These results show which implementation details are co-adapted and co-evolved with algorithms, and which are transferable across algorithms: as examples, we identified that tanh policy and network sizes are highly adapted to algorithmic types, while layer normalization and ELU are critical for MPO’s performances but also transfer to noticeable gains in SAC. We hope our work can inspire future work to further demystify sources of performance improvements across multiple algorithms and allow researchers to build on one another’s both algorithmic and implementational innovations<sup>1</sup>.

---

<sup>1</sup>The University of Tokyo, Tokyo, Japan <sup>2</sup>University of Alberta, Edmonton, Canada <sup>3</sup>Google Research, Mountain View, USA. Correspondence to: Hiroki Furuta <furuta@weblab.t.u-tokyo.ac.jp>.

<sup>1</sup>The implementation is available at <https://github.com/frt03/inference-based-rl>.

## 1. Introduction

Deep reinforcement learning (RL) has achieved huge empirical successes in both continuous (Lillicrap et al., 2016; Gu et al., 2016) and discrete (Mnih et al., 2013; Hessel et al., 2018) problem settings with on-policy (Schulman et al., 2015; 2017) and off-policy (Fujimoto et al., 2018; Haarnoja et al., 2018a;b) algorithms. Especially in the continuous control domain, interpreting RL as probabilistic inference (Todorov, 2008; Toussaint, 2009) has yielded many kinds of algorithms with strong empirical performances (Levine, 2018; Peters et al., 2010; Rawlik et al., 2012; Fox et al., 2016; Jaques et al., 2017; Haarnoja et al., 2017; Ghasemipour et al., 2020; Hafner et al., 2020).

Recently, there have been a series of off-policy algorithms derived from this perspective for learning policies with function approximations (Abdolmaleki et al., 2018b; Haarnoja et al., 2018a; Peng et al., 2019). Notably, Soft Actor Critic (SAC) (Haarnoja et al., 2018a;b), based on maximum entropy objective and soft Q-function, significantly outperforms on-policy (Schulman et al., 2015; 2017) and off-policy (Lillicrap et al., 2016; Gu et al., 2016; Fujimoto et al., 2018) methods. Maximum a posteriori Policy Optimisation (MPO) (Abdolmaleki et al., 2018b), inspired by Peters et al. (2010), employs a pseudo-likelihood objective, and achieves high sample-efficiency and fast convergence compared to the variety of policy gradient methods (Lillicrap et al., 2016; Schulman et al., 2017; Ciosek & Whiteson, 2020). Similar to MPO, Advantage Weighted Regression (AWR) (Peng et al., 2019), and its variant, Advantage Weighted Actor-Critic (AWAC), also employ the pseudo-likelihood objective weighted by the exponential of advantages, and reports more stable performance than baselines both in online and offline (Levine et al., 2020) settings.

While these inference-based algorithms have similar derivations to each other, their empirical performances have large gaps among them when evaluated on the standard continuous control benchmarks, such as OpenAI Gym (Brockman et al., 2016) or DeepMind Control Suite (Tassa et al., 2018). Critically, as each algorithm has unique low-level implementation design decisions – such as optimizers, policy network

architectures, and value estimation techniques – aside from high-level algorithmic choices, it is difficult to exactly identify the causes of these performance gaps as algorithmic or implementational.

In this paper, we first derive MPO, AWR, and SAC from a single objective function, through either Expectation-Maximization (EM) or KL minimization, mathematically clarifying the algorithmic connections among the recent state-of-the-art off-policy actor-critic algorithms. This unified derivation allows us to precisely identify implementation techniques for each algorithm, which are residual design choices in each method that are generally transferable to other algorithms. To reveal the sources of the performance gaps, we experiment with carefully-selected ablations of these identified implementation techniques, such as tanh-squashed action distribution, network architectures, and clipped double Q-learning (Fujimoto et al., 2018). Specifically, we keep the high-level algorithmic designs while normalizing the implementation designs, enabling proper algorithmic comparisons. Our empirical results successfully distinguish between highly co-adapted design choices and no-co-adapted ones. We identified that clipped double Q-learning and tanh-squashed policies, the sources of SoTA performance of SAC, are highly co-adapted to KL-minimization-based method, SAC, and difficult to transfer and benefit in EM-based methods, MPO or AWR. In contrast, we discover that ELU (Clevert et al., 2016) and layer normalization (Ba et al., 2016), the sources of SoTA performance of MPO, are transferable implementation choices from MPO that also significantly benefit SAC. We hope our work can inspire more future works to precisely decouple algorithmic innovations from implementation details, which allows exact sources of performance gains to be identified and algorithmic researches to better build on one another.

## 2. Related Work

**Inference-based RL algorithms** RL as probabilistic inference has been studied in several prior contexts (Todorov, 2008; Toussaint, 2009; Levine, 2018; Fellows et al., 2019; Tang & Kucukelbir, 2020; O’Donoghue et al., 2020), but many recently-proposed algorithms (Abdolmaleki et al., 2018b; Haarnoja et al., 2018a; Peng et al., 2019) are derived separately and their exact relationships are difficult to get out directly, due to mixing of algorithmic and implementational details, inconsistent implementation choices, environment-specific tunings, and benchmark differences. Our work organizes them as a unified policy iteration method, to clarify their exact mathematical algorithmic connections and tease out subtle, but important, implementation differences. We center our analyses around MPO, AWR, and SAC, because they are representative algorithms that span both EM-based (Peters & Schaal, 2007; Peters et al., 2010;

Neumann et al., 2011; Norouzi et al., 2016; Abdolmaleki et al., 2018a; Song et al., 2020; Nair et al., 2020) and KL-control-based (Todorov et al., 2006; Rawlik et al., 2012; Fox et al., 2016; Jaques et al., 2017; Haarnoja et al., 2017; Lee et al., 2020) RL and achieve some of the most competitive performances on popular benchmarks (Brockman et al., 2016; Tassa et al., 2018). REPS (Peters et al., 2010), an EM approach, inspired MPO, AWR, and our unified objective in Equation 1, while Soft Q-learning (Haarnoja et al., 2017), a practical extension of KL control to continuous action space through Liu & Wang (2016), directly led to the development of SAC.

**Meta analyses of RL algorithms** While many papers propose novel algorithms, some recent works focused on meta analyses of some of the popular algorithms, which attracted significant attention due to these algorithms’ high-variance evaluation performances, reproducibility difficulty (Duan et al., 2016; Islam et al., 2017; Wang et al., 2019), and frequent code-level optimizations (Henderson et al., 2017; Tucker et al., 2018; Engstrom et al., 2019; Andrychowicz et al., 2021). Henderson et al. (2017) empirically showed how these RL algorithms have inconsistent results across different official implementations and high variances even across runs with the same hyper-parameters, and recommended a concrete action item for the community – use more random seeds. Tucker et al. (2018) show that high performances of action-dependent baselines (Gu et al., 2017; Grathwohl et al., 2017; Liu et al., 2017; Wu et al., 2018) were more directly due to different subtle implementation choices. Engstrom et al. (2019) focus solely on PPO and TRPO, two on-policy algorithms, and discuss how code-level optimizations, instead of the claimed algorithmic differences, actually led more to PPO’s superior performances. Andrychowicz et al. (2021) describes low-level (e.g. hyper-parameter choice, and regularization) and high-level (e.g. policy loss) design choices in on-policy algorithms affects the performance of PPO by showing results of large-scale evaluations.

In contrast to those prior works that mainly focus on on-policy algorithms, PPO and TRPO, and evaluating their implementation details alone, our work focuses on three off-policy algorithms, and more importantly, presents novel mathematical connections among independently-proposed state-of-the-art algorithms. Our experiments prove how *some* implementation choices in Table 1 are co-evolved with algorithmic innovations and/or have non-trivial effects on the performance of off-policy inference-based methods.

## 3. Preliminaries

We consider a Markov Decision Process (MDP) defined by state space  $\mathcal{S}$ , action space  $\mathcal{A}$ , state transition probability

distribution  $p : \mathcal{S} \times \mathcal{A} \times \mathcal{S} \rightarrow [0, \infty)$ , initial state distribution  $p_1 : \mathcal{S} \rightarrow [0, \infty)$ , reward function  $r : \mathcal{S} \times \mathcal{A} \rightarrow \mathbb{R}$ , and discount factor  $\gamma \in [0, 1)$ . Let  $R_t$  denote a discounted return  $\sum_{u=t}^{\infty} \gamma^{u-t} r(s_u, a_u)$ . We assume the standard RL setting, where the agent chooses actions based on a parametric policy  $\pi_\theta$  and seeks for its parameter that maximizes the expected return  $\mathbb{E}_{\pi_\theta}[R_1]$ . Value functions for a policy  $\pi$  are the expected return conditioned by a state-action pair or a state, that is,  $Q^\pi(s_t, a_t) := \mathbb{E}_\pi[R_t | s_t, a_t]$ , and  $V^\pi(s_t) := \mathbb{E}_\pi[R_t | s_t]$ . They are called the state-action-value function (Q-function), and state-value function, respectively. The advantage function is defined as  $A^\pi(s, a) := Q^\pi(s, a) - V^\pi(s)$ . The Q-function for a policy  $\pi$  is known to be a unique fixed point of the Bellman operator  $\mathcal{T}^\pi$  defined by  $\mathcal{T}^\pi Q(s, a) = r(s, a) + \int \pi(a' | s') p(s' | s, a) Q(s', a') ds' da'$  for any function  $Q : \mathcal{S} \times \mathcal{A} \rightarrow \mathbb{R}$ . We denote a trajectory or successive state-action sequence as  $\tau := (s_1, a_1, s_2, a_2, \dots)$ . We also define an unnormalized state distribution under the policy  $\pi$  by  $d_\pi(s) = \sum_{t=1}^{\infty} \gamma^t p(s_t = s | \pi)$ .

**Inference-based Methods** For simplicity, we consider a finite-horizon MDP with a time horizon  $T$  for the time being. As a result, a trajectory  $\tau$  becomes a finite length:  $\tau := (s_1, a_1, \dots, s_{T-1}, a_{T-1}, s_T)$ .

As in previous works motivated by probabilistic inference (Levine, 2018; Abdolmaleki et al., 2018b), we introduce to the standard graphical model of an MDP a binary event variable  $\mathcal{O}_t \in \{0, 1\}$ , which represents whether the action in time step  $t$  is *optimal* or not. To derive the RL objective, we consider the marginal log-likelihood  $\log \Pr(\mathcal{O} = 1 | \pi_p)$ , where  $\pi_p$  is a policy. Note that  $\mathcal{O} = 1$  means  $\mathcal{O}_t = 1$  for every time step. As is well known, we can decompose this using a variational distribution  $q$  of a trajectory as follows:

$$\begin{aligned} & \log \Pr(\mathcal{O} = 1 | \pi_p) \\ &= \mathbb{E}_q \left[ \log \Pr(\mathcal{O} = 1 | \tau) - \log \frac{q(\tau)}{p(\tau)} + \log \frac{q(\tau)}{p(\tau | \mathcal{O} = 1)} \right] \\ &= \mathcal{J}(p, q) + D_{KL}(q(\tau) || p(\tau | \mathcal{O} = 1)), \end{aligned}$$

where  $\mathcal{J}(p, q)$  is the evidence lower bound (ELBO) defined as  $\mathbb{E}_q[\log \Pr(\mathcal{O} = 1 | \tau)] - D_{KL}(q(\tau) || p(\tau))$ . Inference-based methods aim to find the parametric policy which maximizes the ELBO  $\mathcal{J}(p, q)$ .

There are several algorithmic design choices for  $q$  and  $\Pr(\mathcal{O} = 1 | \tau)$ . Since any  $q$  is valid, a popular choice is the one that factorizes in the same way as  $p$ , that is,

$$\begin{cases} p(\tau) = p(s_1) \prod_t p(s_{t+1} | s_t, a_t) \pi_p(a_t | s_t) \\ q(\tau) = p(s_1) \prod_t p(s_{t+1} | s_t, a_t) \pi_q(a_t | s_t), \end{cases}$$

where  $\pi_p$  is a prior policy, and  $\pi_q$  is a variational posterior policy. We may also choose which policy ( $\pi_p$  or  $\pi_q$ )

to parameterize. As for  $\Pr(\mathcal{O} = 1 | \tau)$ , the most popular choice is the following one (Haarnoja et al., 2017; 2018a; Abdolmaleki et al., 2018b; Levine, 2018; Peng et al., 2019):

$$\Pr(\mathcal{O} = 1 | \tau) \propto \exp \left( \frac{\sum_{t=1}^T \mathcal{G}(s_t, a_t)}{\eta} \right),$$

where  $\eta > 0$  is a temperature, and  $\mathcal{G}$  is a function over  $\mathcal{S} \times \mathcal{A}$ , such as an immediate reward function  $r$ , Q-function  $Q^\pi$ , and advantage function  $A^\pi$ . While we employ  $\exp(\cdot)$  in the present paper, there are alternatives (Oh et al., 2018; Okada & Taniguchi, 2019; Siegel et al., 2020; Wang et al., 2020): for example, Siegel et al. (2020) and Wang et al. (2020) consider an indicator function  $f : x \in \mathbb{R} \mapsto \mathbb{1}[x \geq 0]$ , whereas Oh et al. (2018) considers the rectified linear unit  $f : x \in \mathbb{R} \mapsto \max\{x, 0\}$ .

Incorporating these design choices, we can rewrite the ELBO  $\mathcal{J}(p, q)$  in a more explicit form as

$$\mathcal{J}(\pi_p, \pi_q) = \sum_{t=1}^T \mathbb{E}_q \left[ \frac{\mathcal{G}(s_t, a_t)}{\eta} - D_{KL}(\pi_q(\cdot | s_t) || \pi_p(\cdot | s_t)) \right].$$

In the following section, we adopt this ELBO and consider its relaxation to the infinite-horizon setting. Then, starting from it, we derive MPO, AWR, and SAC.

#### 4. A Unified View of Inference-based Off-Policy Actor-Critic Algorithms

In Section 3, we provided the explicit form of the ELBO  $\mathcal{J}(\pi_p, \pi_q)$ . However, in practice, it is difficult to maximize it as the expectation  $\mathbb{E}_q$  depends on  $\pi_q$ . Furthermore, since we are interested in a finite-horizon setting, we replace  $\sum_{t \in [T]} \mathbb{E}_q$  with  $\mathbb{E}_{d_\pi(s)}$ . Note that the latter expectation  $\mathbb{E}_{d_\pi(s)}$  is taken with the unnormalized state distribution  $d_\pi$  under an arbitrary policy  $\pi$ . This is commonly assumed in previous works (Abdolmaleki et al., 2018b; Haarnoja et al., 2018a). This relaxation leads to the following optimization:

$$\begin{aligned} & \max_{\pi_p, \pi_q} \mathcal{J}(\pi_p, \pi_q) \text{ s.t. } \int d_\pi(s) \int \pi_p(a | s) da ds = 1 \\ & \text{and } \int d_\pi(s) \int \pi_q(a | s) da ds = 1, \end{aligned} \quad (1)$$

where  $\mathcal{J}(\pi_p, \pi_q) = \mathbb{E}_{d_\pi(s)}[\mathcal{G}(s, a)/\eta - D_{KL}(\pi_q || \pi_p)]$ . With this objective, we can regard recent popular SoTA off-policy algorithms, MPO (Abdolmaleki et al., 2018b), AWR (Peng et al., 2019), and SAC (Haarnoja et al., 2018a) as variants of a unified policy iteration method. The components are summarized in Table 1. We first explain how these algorithms can be grouped into two categories of approaches for solving Equation 1, and then we elaborate additional implementation details each algorithm makes.

Method	Algorithm		Implementation				
	$\pi_q$	$\pi_p$	$\pi_q$ update	$\pi_p$ update	$\mathcal{G}$	$\mathcal{G}$ estimate	$\pi_\theta$
MPO	Non-parametric	$\pi_\theta$	Analytic + TR	SG + TR	$Q^{\pi_p}$	Retrace(1)	$\mathcal{N}(\mu_\theta(s), \Sigma_\theta(s))$
AWR	Non-parametric	$\pi_\theta$	Analytic	Mixture + SG	$A^{\pi_p}$	TD( $\lambda$ )	$\mathcal{N}(\mu_\theta(s), \Sigma)$
AWAC	Non-parametric	$\pi_\theta$	Analytic	Mixture + SG	$Q^{\pi_p}$	TD(0)	$\mathcal{N}(\mu_\theta(s), \Sigma_\theta)$
SAC		Fixed	SG	(Fixed to Unif.)	$Q_{\text{soft}}^{\pi_q}$	TD(0) + TD3	$\text{Tanh}(\mathcal{N}(\mu_\theta(s), \Sigma_\theta(s)))$
PoWER	Non-parametric	$\pi_\theta$	Analytic	Analytic	$\eta \log Q^{\pi_p}$	TD(1)	$\mathcal{N}(\mu_\theta(s), \Sigma_\theta(s))$
RWR	Non-parametric	$\pi_\theta$	Analytic	SG	$\eta \log r$	–	$\mathcal{N}(\mu_\theta(s), \Sigma)$
REPS	Non-parametric	$\pi_q$	Analytic	$\pi_q$	$A^{\pi_p}$	TD(0)	Softmax
UREX	Non-parametric	$\pi_\theta$	Analytic	SG	$Q^{\pi_p}$	TD(1)	Softmax
V-MPO	Non-parametric	$\pi_\theta$	Analytic + TR	SG + TR	$A^{\pi_p}$	$n$ -step TD	$\mathcal{N}(\mu_\theta(s), \Sigma_\theta(s))$
TRPO		$\pi_q$	TR	$\pi_q$	$A^{\pi_p}$	TD(1)	$\mathcal{N}(\mu_\theta(s), \Sigma_\theta)$
PPO		$\pi_q$	SG + TR	$\pi_q$	$A^{\pi_p}$	GAE	$\mathcal{N}(\mu_\theta(s), \Sigma_\theta)$
DDPG*		Fixed	SG	(Fixed)	$Q^{\pi_q}$	TD(0)	$\mu_\theta(s)$
TD3*		Fixed	SG	(Fixed)	$Q^{\pi_q}$	TD(0) + TD3	$\mu_\theta(s)$

Table 1. Taxonomy based on the components of inference-based off-policy algorithms: MPO (Abdolmaleki et al., 2018b), AWR (Peng et al., 2019), AWAC (Nair et al., 2020), SAC (Haarnoja et al., 2018a), and other algorithms (see Appendix C for the details). We follow the notation of Section 3 and 4. We characterize them with seven factors, the parameterization of the policy ( $\pi_q$  and  $\pi_p$ ), how policies are updated ( $\pi_q$  and  $\pi_p$ ), the choice of  $\mathcal{G}(\cdot)$ , how  $\mathcal{G}$  is estimated, and the distribution of the policy. While the advantage function just can be interpreted as Q-function with baseline subtraction, we explicitly write  $A^\pi$  when the state-value function is parameterized instead of Q-function. (\*Note that DDPG and TD3 are not the “inference-based” algorithms, but we can classify these two as KL control variants.)

#### 4.1. Unified Policy Iteration: Algorithmic Perspective

Equation 1 allows the following algorithmic choices: how or if to parameterize  $\pi_p$  and  $\pi_q$ ; what optimizer to use for them; and if to optimize them jointly, or individually while holding the other fixed. We show that the algorithms in Table 1 can be classified into two categories: Expectation-Maximization control (EM control) and direct Kullback-Leibler divergence minimization control (KL control).

##### 4.1.1. EXPECTATION-MAXIMIZATION (EM) CONTROL

This category subsumes MPO (Abdolmaleki et al., 2018b) (similarly, REPS (Peters et al., 2010)), AWR (Peng et al., 2019), and AWAC (Nair et al., 2020), and we term it *EM control*. At high level, the algorithm non-parametrically solves for the variational posterior  $\pi_q$  while holding the parametric prior  $\pi_p = \pi_{\theta_p}$  fixed (E-Step), and then optimize  $\pi_p$  holding the new  $\pi_q$  fixed (M-Step). This can be viewed as either a generic EM algorithm and as performing coordinate ascent on Equation 1. We denote  $\theta_p$  and  $\pi_q$  after iteration  $k$  of EM steps by  $\theta_p^{(k)}$  and  $\pi_q^{(k)}$ , respectively.

In **E-step** at iteration  $k$ , we force the variational posterior policy  $\pi_q^{(k)}$  to be close to the optimal posterior policy, i.e., the maximizer of the ELBO  $\mathcal{J}(\pi_{\theta_p^{(k-1)}}, \pi_q)$  with respect to  $\pi_q$ . EM control converts the hard-constraint optimization

problem in Equation 1 to solving the following Lagrangian,

$$\begin{aligned} \mathcal{J}(\pi_q, \beta) = & \int d_\pi(s) \int \pi_q(a|s) \frac{\mathcal{G}(s, a)}{\eta} \\ & - \int d_\pi(s) \int \pi_q(a|s) \log \frac{\pi_q(a|s)}{\pi_{\theta_p^{(k-1)}}(a|s)} d a d s \\ & + \beta \left( 1 - \int d_\pi(s) \int \pi_q(a|s) d a d s \right). \end{aligned} \quad (2)$$

We analytically obtain the solution of Equation 2,

$$\pi_q^{(k)}(a|s) = \frac{1}{Z(s)} \pi_{\theta_p^{(k-1)}}(a|s) \exp\left(\frac{\mathcal{G}(s, a)}{\eta}\right),$$

where  $Z(s)$  is the partition function.

In **M-Step** at iteration  $k$ , we maximize the ELBO  $\mathcal{J}(\pi_q^{(k)}, \pi_p)$  with respect to  $\pi_p$ . Considering the optimization with respect to  $\pi_p$  in Equation 1 results in *forward* KL minimization, which is often referred to as a pseudo-likelihood or policy projection objective,

$$\begin{aligned} \max_{\theta_p} \mathbb{E}_{d_\pi(s) \pi_q^{(k)}(a|s)} [\log \pi_{\theta_p}(a|s)] \\ = \max_{\theta_p} \mathbb{E}_{d_\pi(s) \pi_{\theta_p^{(k-1)}}(a|s)} \left[ \frac{\log \pi_{\theta_p}(a|s)}{Z(s)} \exp\left(\frac{\mathcal{G}(s, a)}{\eta}\right) \right], \end{aligned} \quad (3)$$

where  $Z(s)$  is estimated with  $M$  action samples in practice;  $Z(s) \approx \frac{1}{M} \sum_{j=1}^M \exp(\mathcal{G}(s, a_j)/\eta)$  with  $a_j \sim \pi_{\theta_p^{(k-1)}}(\cdot|s)$ .

##### 4.1.2. DIRECT KULLBACK-LEIBLER (KL) DIVERGENCE MINIMIZATION CONTROL

In contrast to the EM control in Section 4.1.1, we only optimize the variational posterior  $\pi_q$  while holding the prior  $\pi_p$  fixed. In this scheme,  $\pi_q$  is parameterized, so we denote

it as  $\pi_{\theta_q}$ . This leads to *KL control* (Todorov et al., 2006; Toussaint & Storkey, 2006; Rawlik et al., 2012; Fox et al., 2016; Jaques et al., 2017; Haarnoja et al., 2017).

Equivalent to E-step in Section 4.1.1, we force the variational posterior policy  $\pi_{\theta_q}$  to be close to the optimal posterior policy, i.e, the maximizer of  $\mathcal{J}(\pi_p, \pi_q)$  with respect to  $\pi_q$ . The difference is that instead of analytically solving  $\mathcal{J}(\pi_p, \pi_q)$  for  $\pi_q$ , we optimize  $\mathcal{J}(\pi_p, \pi_{\theta_q})$  with respect to  $\theta_q$ , which results in the following objective,

$$\max_{\theta_q} \mathbb{E}_{d_{\pi}(s)\pi_{\theta_q}(a|s)} \left[ \frac{\mathcal{G}(s, a)}{\eta} - \log \frac{\pi_{\theta_q}(a|s)}{\pi_p(a|s)} \right].$$

#### 4.1.3. “OPTIMAL” POLICIES OF EM AND KL CONTROL

While we formulate EM and KL control in a unified framework, we note that they have a fundamental difference in their definition of “optimal” policies. KL control fixes  $\pi_p$  and converges to a *regularized-optimal* policy in an exact case (Geist et al., 2019; Vieillard et al., 2021). In contrast, EM control continues updating both  $\pi_p$  and  $\pi_q$ , resulting in convergence to the *standard optimal* policy in an exact case (Rawlik et al., 2012). We also note that EM control solves KL control as a sub-problem; for example, the first E-step exactly corresponds to a KL control problem, except the policy parameterization.

## 4.2. Unified Policy Iteration: Implementation Details

In this section, we explain the missing pieces of MPO, AWR, and SAC in Section 4.1. Additionally, we also describe the details of other algorithms (Kober & Peters, 2008; Peters & Schaal, 2007; Peters et al., 2010; Nachum et al., 2017; Song et al., 2020; Lillicrap et al., 2016; Fujimoto et al., 2018; Schulman et al., 2015; 2017) from the EM and KL control perspective. See Appendix C for the details.

### 4.2.1. MPO

**Algorithm** MPO closely follows the EM control scheme explained in Section 4.1.1, wherein  $\pi_p = \pi_{\theta_p}$  is parametric, and  $\pi_q$  is non-parametric.

**Implementation [ $\pi_q$  Update]** This corresponds to the E-step. MPO uses a trust-region (TR) method. Concretely, it replaces the reverse KL penalty (second term) in the Lagrangian (Equation 2) with a reverse KL constraint and analytically solves it for  $\pi_q$ . As a result,  $\eta$  is also optimized during the training by minimizing the dual of Equation 2,

$$g(\eta) = \eta\epsilon + \eta \log \mathbb{E}_{d_{\pi}(s)\pi_{\theta_p^{(k-1)}}(a|s)} \left[ \exp \left( \frac{Q^{\pi_{\theta_p^{(k-1)}}}(s, a)}{\eta} \right) \right].$$

This constraint by a reverse KL in the E-step and the optimization of  $\eta$  resemble REPS (Peters et al., 2010).

**[ $\pi_p$  Update]** This corresponds to the M-step. MPO uses a combination of Stochastic Gradient (SG) ascent and trust-region method based on a forward KL divergence similarly to TRPO (Schulman et al., 2015). Concretely, it obtains  $\theta_p^{(k)}$  by maximizing the objective (Equation 3) with respect to  $\theta_p$  subject to  $\mathbb{E}_{d_{\pi}(s)}[D_{KL}(\pi_{\theta_p^{(k-1)}}(\cdot|s) || \pi_{\theta_p}(\cdot|s))] \leq \epsilon$ . MPO further decompose this KL divergence to two terms, assuming Gaussian policies; one term includes only the mean vector of  $\pi_{\theta_p}(\cdot|s)$ , and the other includes only its covariance matrix. Abdolmaleki et al. (2018b) justify this as a log-prior of MAP estimation, which is assumed as a second-order approximation of KL divergence.

**[ $\mathcal{G}$  and  $\mathcal{G}$  Estimate]** MPO uses the Q-function of  $\pi_{\theta_p^{(k-1)}}$  as  $\mathcal{G}$  in the  $k$ -th E-step. Abdolmaleki et al. (2018b) originally use the Retrace update (Munos et al., 2016), while their practical implementation (Hoffman et al., 2020) uses a single-step Bellman update.

**[ $\pi_{\theta}$ ]** For a parameterized policy, MPO uses a Gaussian distribution with state-dependent mean vector and diagonal covariance matrix. The trust-region method in MPO’s M-step heavily relies on this Gaussian assumption. Since a Gaussian distribution has an infinite support, MPO has a penalty term in its policy loss function that forces the mean of the policy to stay within the range of action space.

### 4.2.2. AWR AND AWAC

**Algorithm** AWR slightly deviates from the EM control. In the M-step, AWR ignores  $Z(s)$  and simply set it to 1.

**Implementation [ $\pi_q$  Update]** This corresponds the E-step. AWR and AWAC analytically solves the Lagrangian (Equation 2). In contrast to MPO, they don’t use trust-region method.

**[ $\pi_p$  Update]** This corresponds to the M-step. At iteration  $k$ , AWR uses an average of all previous policies  $\tilde{\pi}_{p^k} := \frac{1}{k} \sum_{j=0}^{k-1} \pi_{\theta_p^{(j)}}$  instead of  $\pi_{\theta_p^{(k-1)}}$  (cf. Equation 3). In practice, the average policy  $\tilde{\pi}_p$  is replaced by samples of actions from a replay buffer, which stores action samples of previous policies  $\pi_{\theta_p^{(j)}}$ .

**[ $\mathcal{G}$  and  $\mathcal{G}$  Estimate]** AWR uses the advantage function of  $\tilde{\pi}_{p^k}$  as  $\mathcal{G}$  in the  $k$ -th E-step. AWR learns the state value function of  $\pi_{\theta_p^{(k-1)}}$  with TD( $\lambda$ ) (Schulman et al., 2016). Due to its choice of  $\tilde{\pi}_{p^k}$ , this avoids importance corrections (Munos et al., 2016). AWAC (Nair et al., 2020) updates the policies similarly, but the advantage is estimated via the Q-function instead of the state-value function in AWR, and with TD(0).

$[\pi_\theta]$  For a parameterized policy, both AWR and AWAC use a Gaussian distribution with a state-dependent mean vector and a state-independent diagonal covariance matrix (AWR uses a constant one). As in MPO, AWR and AWAC uses a penalty term to keep the mean of the policy within the range of action space.

#### 4.2.3. SAC

**Algorithm** Contrary to MPO and AWR, SAC follows the KL control scheme explained in Section 4.1.2, wherein the variational posterior policy  $\pi_q = \pi_{\theta_q}$  is parameterized, and the prior policy  $\pi_p$  is fixed to the uniform distribution over the action space  $\mathcal{A}$ . SAC uses as  $\mathcal{G}$  a soft Q-function:

$$Q_{\text{soft}}^{\pi_{\theta_q}}(s_t, a_t) := r(s_t, a_t) + \gamma \mathbb{E}_{\pi_{\theta_q}} \left[ V_{\text{soft}}^{\pi_{\theta_q}}(s_{t+1}) \right],$$

where

$$\begin{aligned} V_{\text{soft}}^{\pi_{\theta_q}}(s_t) \\ := V^{\pi_{\theta_q}}(s_t) + \mathbb{E}_{\pi_{\theta_q}} \left[ \sum_{u=t}^{\infty} \gamma^{u-t} \eta \mathcal{H}(\pi_{\theta_q}(\cdot | s_t)) | s_t \right] \end{aligned}$$

with  $\mathcal{H}(\pi_{\theta_q}(\cdot | s_t))$  being  $-\mathbb{E}_{\pi_{\theta_q}} [\log \pi_{\theta_q}(a_t | s_t) | s_t]$ .

**Implementation  $[\pi_q$  and  $\pi_p$  Update]** SAC performs stochastic gradient (SG) ascent updates of only  $\pi_q$ , where the objective function is shown in Equation 1. SAC has no operation equivalent to M-step in MPO and AWR, since it keeps the prior policy  $\pi_p$  to the uniform distribution.

Similar to the temperature tuning in MPO, Haarnoja et al. (2018b) consider the dual function of entropy constrained Lagrangian and treat the temperature  $\eta$  as a Lagrange multiplier, which results in,

$$g(\eta) = -\eta \bar{\mathcal{H}} - \eta \mathbb{E}_{d_{\pi(s)} \pi_{\theta_q}(a|s)} [\log \pi_{\theta_q}(a|s)],$$

where  $\bar{\mathcal{H}}$  is the target entropy to ensure that the entropy of the policy should be larger than it.

**$[\mathcal{G}$  and  $\mathcal{G}$  Estimate]** SAC uses  $Q_{\text{soft}}^{\pi_{\theta_q}}$  as  $\mathcal{G}$ . In particular, it uses TD(0)-like algorithm based on this soft Q-function.

In policy evaluation, clipped double Q-learning (Fujimoto et al., 2018), which retains multiple Q-functions (typically two) and takes the minimum, is employed as a stabilization method to suppress the overestimation of Q value.

$[\pi_\theta]$  The policy of SAC is a squashed Gaussian distribution: SAC first samples a random variable  $u$  from a Gaussian distribution  $\mathcal{N}(\mu_\theta(s), \Sigma_\theta(s))$  with state-dependent mean vector and diagonal covariance; then, it applies the tanh function to  $u$  and obtain the action  $a \in [-1, 1]^{|\mathcal{A}|}$ . (If a dimension of the action space is not  $[-1, 1]$ , an appropriate scaling and shift by an affine function is applied after the squashing.) Tanh squashing prevents out-of-bounds action.

### 4.3. Empirical Comparison

To evaluate the empirical performance of these off-policy algorithms (MPO, AWR, AWAC, and SAC), we compare their performances on Open AI Gym MuJoCo environments, namely, Hopper, Walker2d, HalfCheetah, Ant, Humanoid, and Swimmer, following Haarnoja et al. (2018b). We use the implementation of SAC reproduced in PFRL (Fujita et al., 2019), and implement AWR and MPO based on it referring their original implementations (Peng et al., 2019; Nair et al., 2020; Hoffman et al., 2020) (see Appendix D for the reproduction results of AWR).

Figure 1 shows that SAC outperforms MPO, AWR, and AWAC in four environments (Hopper, Walker2d, HalfCheetah, and Humanoid), while MPO in Ant and AWR in Swimmer achieves the best performance. Generally, SAC seems to perform consistently better in these locomotion tasks. We extensively evaluate MPO, AWR, and SAC on the 3 manipulation tasks and 28 tasks on DeepMind Control Suite. See Appendix B and G for the details.

## 5. Identifying Co-Adaptation of Algorithmic and Implementational Innovations

In Section 4.3, SAC shows the notable results in most of environments, while the derivation and formulation of those methods resemble to each other. To specify the source of performance gaps except for their mathematical differences, we experiment with some ablations focusing on (1) clipped double Q-learning, (2) the distribution of the policy, (3) network architectures (4) ELU and layer normalization, stabilization techniques in MPO.

### 5.1. Clipped Double Q-Learning

We hypothesize that clipped double Q-learning has a large effect on the notable performance of SAC, and can be transferable in EM control methods. To verify this, we test the effect of clipped double Q-learning. Instead of AWR, here we evaluate AWAC since it uses Q-function.

Table 2 shows that single-Q SAC outperforms original one in HalfCheetah and Swimmer that do not have the termination of the episode, while struggles to learn in Hopper, Walker, Ant and Humanoid that have the episodic termination conditions. A hypothesis is that single-Q SAC obtains a more exploratory policy due to larger overestimation bias, which can help in environments where explorations are safe, but hurt in environments where reckless explorations lead to immediate episode terminations. On the other hand, clipped double Q-learning does not affect MPO or AWAC performances as significantly as SAC, where most results do not change and only few lead to small improvements over the original ones. This suggests that clipped double Q-learning

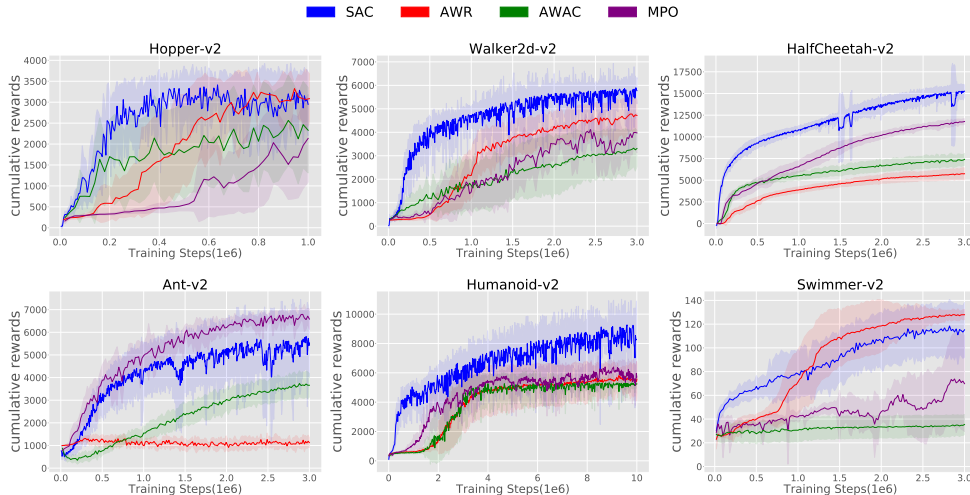


Figure 1. Benchmarking results on OpenAI Gym MuJoCo locomotion environments. All methods are run with 10 random seeds. SAC seems to perform consistently better.

	SAC (D)	SAC (S)	AWAC (D)	AWAC (S)	MPO (D)	MPO (S)
Hopper-v2	<b>3013 ± 602</b>	1601 ± 733	2329 ± 1020	2540 ± 755	2352 ± 959	2136 ± 1047
Walker2d-v2	<b>5820 ± 411</b>	1888 ± 922	3307 ± 780	3662 ± 712	4471 ± 281	3972 ± 849
HalfCheetah-v2	15254 ± 751	<b>15701 ± 630</b>	7396 ± 677	7226 ± 449	12028 ± 191	11769 ± 321
Ant-v2	5532 ± 1266	1163 ± 1326	3659 ± 523	3008 ± 375	<b>7179 ± 190</b>	6584 ± 455
Humanoid-v2	<b>8081 ± 1149</b>	768 ± 215	5243 ± 200	2738 ± 982	6858 ± 373	5709 ± 1081
Swimmer-v2	114 ± 21	<b>143 ± 3</b>	35 ± 8	38 ± 7	69 ± 29	70 ± 40

Table 2. Ablation of Clipped Double Q-Learning. (D) denotes algorithms with clipped double Q-learning, and (S) denotes without it. We test original SAC (D), AWAC (D), MPO (S) and some variants; SAC without clipped double Q (S), AWAC (S), and MPO with clipped double Q (D). SAC (S) beats SAC (D) in HalfCheetah and Swimmer, while it fails in Hopper, Walker, Ant and Humanoid, which implies that SAC (S) obtains a highly exploratory policy, since it fails in termination environments. The learning curves are shown in Appendix F.

might be a co-dependent choices to KL control methods.

## 5.2. The distribution of the policy

To validate the effect of tanh-squashed action distribution (last column in Table 1), we compare SAC without tanh transform (using MPO action penalty instead) to the original one, which results in drastic degradation (Table 3). This degeneration can be caused by the maximum entropy objective that encourages the maximization of the covariance. These observations suggest that the high performance of SAC seems to depend on the implementational choice of the policy distribution. In contrast, MPO and AWR with tanh squashing cause numerical instability, which ends up with NaN outputs. This also suggests that tanh-squashed policy might be highly co-adapted in SAC and not be transferable to EM control methods due to its instability.

## 5.3. Network Architectures

While on-policy algorithms such as PPO and TRPO can use the common network architecture as in prior works (Engstrom et al., 2019; Henderson et al., 2017), the architecture that works well in all the off-policy inference-based methods is not obvious, and the RL community doesn’t have an

agreeable default choice. To validate the dependency of the performance on network architectures in inference-based methods, we exchange the configuration of the policy and value networks; namely, the size and number of hidden layers, the type of activation function, network optimizer and its learning rate, weight-initialization, and the normalization of input state (see Table 4 in Appendix A). All other components remain the original implementations. Figure 2 illustrates that the originally proposed architectures of each algorithm archive better performances and the swapped architectures do not show the notable results, except for some combinations, such as SAC(Net: MPO) in Ant, HalfCheetah, Humanoid, and AWR variants in Swimmer. These results suggest that these off-policy inference-based algorithms might be fragile with other network architectures and more co-dependent with architectures than on-policy algorithms. Our experiments also highlight a non-trivial and important future research direction: What architectures can work reasonably in all the off-policy inference-based methods, and be used as a basis for large-scale code-level investigations such as those done for on-policy methods (Andrychowicz et al., 2021)?

	SAC (w/)	SAC (w/o)	AWR (w/)	AWR (w/o)	MPO (w/)	MPO (w/o)
Hopper-v2	3013 ± 602	6 ± 10	<b>3267 ± 383</b>	3085 ± 593	301 ± 12 <sup>†</sup>	2136 ± 1047
Walker2d-v2	<b>5820 ± 411</b>	−∞	3281 ± 1084 <sup>†</sup>	4717 ± 678	328 ± 95 <sup>†</sup>	3972 ± 849
HalfCheetah-v2	<b>15254 ± 751</b>	−∞	1159 ± 599 <sup>†</sup>	5742 ± 667	831 ± 242 <sup>†</sup>	11769 ± 321
Ant-v2	5532 ± 1266	−∞	152 ± 101 <sup>†</sup>	1127 ± 224	202 ± 102 <sup>†</sup>	<b>6584 ± 455</b>
Humanoid-v2	<b>8081 ± 1149</b>	108 ± 82 <sup>†</sup>	538 ± 49 <sup>†</sup>	5573 ± 1020	5642 ± 77 <sup>†</sup>	5709 ± 1081
Swimmer-v2	114 ± 21	28 ± 11	117 ± 16	<b>128 ± 4</b>	37 ± 6 <sup>†</sup>	70 ± 40

Table 3. Ablation of Tanh transformation (<sup>†</sup>numerical error happens during training). We test SAC without tanh squashing, AWR with tanh, and MPO with tanh. SAC without tanh transform results in drastic degradation of the performance, which can be caused by the maximum entropy objective that encourages the maximization of the covariance. The learning curves are shown in Appendix F.

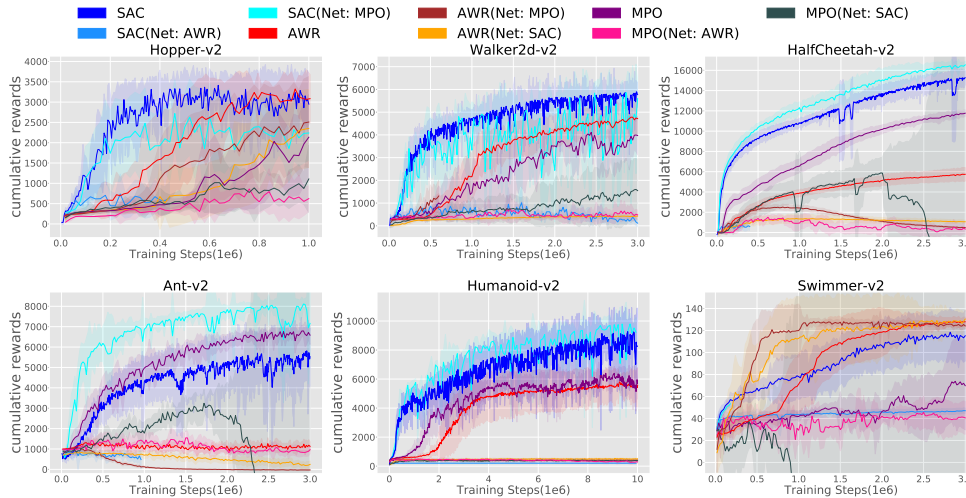


Figure 2. Swapping network architectures between each methods. These results suggest that these off-policy inference-based algorithms might be fragile with other network architectures and more co-dependent with architectures than on-policy algorithms. A line that stops in the middle means that training has stopped at that step with numerical error due to NaN outputs. See Appendix E for the detailed scores.

#### 5.4. ELU and Layer Normalization

The implementation of MPO (Hoffman et al., 2020) has some code-level implementation details, ELU activation (Clevert et al., 2016) and layer normalization (Ba et al., 2016), that stabilize the learning process. We hypothesize that these design choices contribute the performance of MPO most, especially in Ant in Section 4.3, since SAC with MPO architecture shows a significant gain in Section 5.3. To investigate this much deeper, we add ELU and layer normalization into SAC, and remove them from MPO while keeping the rest of the original implementation.

Figure 3 shows that layer normalization can contribute to a significantly higher performance of SAC in Ant, and replacing ReLU with ELU also improves performance a lot in Swimmer, where AWR is the best algorithm in Figure 1. In contrast, the performance of MPO collapsed when we removed ELU and layer normalization, seemingly small implementations. This observation suggests that these implementations of MPO are less co-adapted to EM control methods only, but are transferable and beneficial to KL control methods. For additional environments, we tested incorporating ELU and layer normalization to SAC in other 4 MuJoCo and 12 DM Control tasks where MPO outper-

formed SAC, and observed that they again often benefit SAC performances substantially and are critical for MPO performances. See Appendix F and G for the details.

As a concluding remark from these experiments, it is important to disentangle implementation choices from algorithmic designs, which can sometimes help us identify overlooked implementation choices that improve the performance even more than algorithmic innovations.

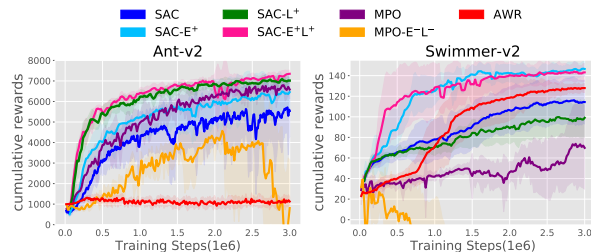


Figure 3. Comparison between original SAC and combination of implementation details in MPO, ELU and layer normalization. E<sup>+</sup>/L<sup>+</sup> indicates adding, and E<sup>-</sup>/L<sup>-</sup> indicates removing ELU/layer normalization. Introducing layer normalization into original SAC (green) significantly improves the performance in Ant, and SAC replacing ReLU with ELU (light blue) performs better in Swimmer. See Appendix F.3 for further details.

## 6. Conclusion

In this work, we present a taxonomy of inference-based algorithms, and successfully identify algorithm-specific as well as algorithm-agnostic implementation details that cause substantial performance improvements. We first reformulated recent inference-based off-policy algorithms – such as MPO, AWR and SAC – into a unified mathematical objective and clarified the algorithmic and implementational differences. Through precise ablation studies, we empirically show that implementation choices like tanh-squashed distribution and clipped double Q-learning are highly co-adapted to KL control methods (e.g. SAC), and difficult to transfer and benefit in EM control methods (e.g. MPO or AWR). As an example, the network architectures of inference-based off-policy algorithms seem more co-dependent than on-policy methods like PPO or TRPO, which therefore have significant impacts on the overall algorithm performances and need to be carefully tuned per algorithm. Such dependence of each algorithmic innovation on specific hand-tuned implementation details makes accurate performance gain attributions and cumulative build-up of research insights difficult. In contrast, we also find that some code-level implementation details, such as ELU and layer normalization, are transferable techniques from MPO and also benefit SAC substantially. We hope our work can encourage more works that study precisely the impacts of algorithmic properties and empirical design choices, not only for one type of algorithms, but also across a broader spectrum of deep RL algorithms.

## Acknowledgements

We thank Yusuke Iwasawa, Masahiro Suzuki, Marc G. Belle-mare, Ofir Nachum, and Sergey Levine for many fruitful discussions and comments.

## References

- Abdolmaleki, A., Springenberg, J. T., Degraeve, J., Bohez, S., Tassa, Y., Belov, D., Heess, N., and Riedmiller, M. Relative entropy regularized policy iteration. *arXiv preprint arXiv:1812.02256*, 2018a.
- Abdolmaleki, A., Springenberg, J. T., Tassa, Y., Munos, R., Heess, N., and Riedmiller, M. Maximum a posteriori policy optimisation. In *International Conference on Learning Representations*, 2018b.
- Andrychowicz, M., Raichuk, A., Stańczyk, P., Orsini, M., Girgin, S., Marinier, R., Hussenot, L., Geist, M., Pietquin, O., Michalski, M., Gelly, S., and Bachem, O. What matters for on-policy deep actor-critic methods? a large-scale study. In *International Conference on Learning Representations*, 2021.
- Ba, J. L., Kiros, J. R., and Hinton, G. E. Layer normalization. *arXiv preprint arXiv:1607.06450*, 2016.
- Brockman, G., Cheung, V., Pettersson, L., Schneider, J., Schulman, J., Tang, J., and Zaremba, W. Openai gym. *arXiv preprint arXiv:1606.01540*, 2016.
- Ciosek, K. and Whiteson, S. Expected policy gradients for reinforcement learning. *Journal of Machine Learning Research*, 2020.
- Clevert, D.-A., Unterthiner, T., and Hochreiter, S. Fast and accurate deep network learning by exponential linear units (elus). In *International Conference on Learning Representations*, 2016.
- Duan, Y., Chen, X., Houthoofd, R., Schulman, J., and Abbeel, P. Benchmarking deep reinforcement learning for continuous control. In *International Conference on Machine Learning*, 2016.
- Engstrom, L., Ilyas, A., Santurkar, S., Tsipras, D., Janoos, F., Rudolph, L., and Madry, A. Implementation matters in deep rl: A case study on ppo and trpo. In *International Conference on Learning Representations*, 2019.
- Fellows, M., Mahajan, A., Rudner, T. G., and Whiteson, S. Virel: A variational inference framework for reinforcement learning. In *Advances in Neural Information Processing Systems*, 2019.
- Fox, R., Pakman, A., and Tishby, N. Taming the noise in reinforcement learning via soft updates. In *Conference on Uncertainty in Artificial Intelligence*, 2016.
- Fujimoto, S., van Hoof, H., and Meger, D. Addressing function approximation error in actor-critic methods. In *International Conference on Machine Learning*, 2018.
- Fujita, Y., Kataoka, T., Nagarajan, P., and Ishikawa, T. Chainerrl: A deep reinforcement learning library. In *Workshop on Deep Reinforcement Learning at the 33rd Conference on Neural Information Processing Systems*, 2019.
- Geist, M., Scherrer, B., and Pietquin, O. A theory of regularized Markov decision processes. In *International Conference on Machine Learning*, 2019.
- Ghasemipour, S. K. S., Zemel, R., and Gu, S. A divergence minimization perspective on imitation learning methods. In *Conference on Robot Learning*, 2020.
- Grathwohl, W., Choi, D., Wu, Y., Roeder, G., and Duvenaud, D. Backpropagation through the void: Optimizing control variates for black-box gradient estimation. *arXiv preprint arXiv:1711.00123*, 2017.

- Gu, S., Lillicrap, T., Sutskever, I., and Levine, S. Continuous deep q-learning with model-based acceleration. In *International Conference on Machine Learning*, 2016.
- Gu, S., Lillicrap, T., Ghahramani, Z., Turner, R. E., and Levine, S. Q-Prop: Sample-efficient policy gradient with an off-policy critic. In *International Conference on Learning Representations*, 2017.
- Haarnoja, T., Tang, H., Abbeel, P., and Levine, S. Reinforcement learning with deep energy-based policies. In *International Conference on Machine Learning*, 2017.
- Haarnoja, T., Zhou, A., Abbeel, P., and Levine, S. Soft actor-critic: Off-policy maximum entropy deep reinforcement learning with a stochastic actor. In *International Conference on Machine Learning*, 2018a.
- Haarnoja, T., Zhou, A., Hartikainen, K., Tucker, G., Ha, S., Tan, J., Kumar, V., Zhu, H., Gupta, A., Abbeel, P., and Levine, S. Soft actor-critic algorithms and applications. *arXiv preprint arXiv:1812.05905*, 2018b.
- Hafner, D., Ortega, P. A., Ba, J., Parr, T., Friston, K., and Heess, N. Action and perception as divergence minimization. *arXiv preprint arXiv:2009.01791*, 2020.
- Henderson, P., Islam, R., Bachman, P., Pineau, J., Precup, D., and Meger, D. Deep reinforcement learning that matters. In *AAAI Conference on Artificial Intelligence*, 2017.
- Hessel, M., Modayil, J., Van Hasselt, H., Schaul, T., Ostrovski, G., Dabney, W., Horgan, D., Piot, B., Azar, M., and Silver, D. Rainbow: Combining improvements in deep reinforcement learning. In *AAAI Conference on Artificial Intelligence*, 2018.
- Hoffman, M., Shahriari, B., Aslanides, J., Barth-Maron, G., Behbahani, F., Norman, T., Abdolmaleki, A., Cassirer, A., Yang, F., Baumli, K., Henderson, S., Novikov, A., Colmenarejo, S. G., Cabi, S., Gulcehre, C., Paine, T. L., Cowie, A., Wang, Z., Piot, B., and de Freitas, N. Acme: A research framework for distributed reinforcement learning. *arXiv preprint arXiv:2006.00979*, 2020.
- Islam, R., Henderson, P., Gomrokchi, M., and Precup, D. Reproducibility of benchmarked deep reinforcement learning tasks for continuous control. *arXiv preprint arXiv:1708.04133*, 2017.
- Jaques, N., Gu, S., Bahdanau, D., Hernández-Lobato, J. M., Turner, R. E., and Eck, D. Sequence tutor: Conservative fine-tuning of sequence generation models with kl-control. In *International Conference on Machine Learning*, 2017.
- Kober, J. and Peters, J. Policy search for motor primitives in robotics. In *Advances in neural information processing systems*, 2008.
- Kumar, A., Fu, J., Soh, M., Tucker, G., and Levine, S. Stabilizing off-policy q-learning via bootstrapping error reduction. In *Advances in Neural Information Processing Systems*, 2019.
- Lee, A. X., Nagabandi, A., Abbeel, P., and Levine, S. Stochastic latent actor-critic: Deep reinforcement learning with a latent variable model. In *Advances in Neural Information Processing Systems*, 2020.
- Levine, S. Reinforcement Learning and Control as Probabilistic Inference: Tutorial and review. *arXiv preprint arXiv:1805.00909*, 2018.
- Levine, S., Kumar, A., Tucker, G., and Fu, J. Offline reinforcement learning: Tutorial, review, and perspectives on open problems. *arXiv preprint arXiv:2005.01643*, 2020.
- Lillicrap, T. P., Hunt, J. J., Pritzel, A., Heess, N., Erez, T., Tassa, Y., Silver, D., and Wierstra, D. Continuous control with deep reinforcement learning. In *International Conference on Learning Representations*, 2016.
- Liu, H., Feng, Y., Mao, Y., Zhou, D., Peng, J., and Liu, Q. Action-dependent control variates for policy optimization via stein's identity. *arXiv preprint arXiv:1710.11198*, 2017.
- Liu, Q. and Wang, D. Stein variational gradient descent: A general purpose bayesian inference algorithm. *arXiv preprint arXiv:1608.04471*, 2016.
- Mnih, V., Kavukcuoglu, K., Silver, D., Graves, A., Antonoglou, I., Wierstra, D., and Riedmiller, M. Playing atari with deep reinforcement learning. *arXiv preprint arXiv:1312.5602*, 2013.
- Munos, R., Stepleton, T., Harutyunyan, A., and Bellemare, M. G. Safe and efficient off-policy reinforcement learning. In *Advances in Neural Information Processing Systems*, 2016.
- Nachum, O., Norouzi, M., and Schuurmans, D. Improving policy gradient by exploring under-appreciated rewards. In *International Conference on Learning Representations*, 2017.
- Nair, A., Dalal, M., Gupta, A., and Levine, S. Accelerating online reinforcement learning with offline datasets. *arXiv preprint arXiv:2006.09359*, 2020.
- Neumann, G. et al. Variational inference for policy search in changing situations. In *International Conference on Machine Learning*, 2011.

- Norouzi, M., Bengio, S., Jaitly, N., Schuster, M., Wu, Y., Schuurmans, D., et al. Reward augmented maximum likelihood for neural structured prediction. In *Advances In Neural Information Processing Systems*, 2016.
- O'Donoghue, B., Osband, I., and Ionescu, C. Making sense of reinforcement learning and probabilistic inference. In *International Conference on Learning Representations*, 2020.
- Oh, J., Guo, Y., Singh, S., and Lee, H. Self-imitation learning. In *International Conference on Machine Learning*, 2018.
- Okada, M. and Taniguchi, T. Variational inference mpc for bayesian model-based reinforcement learning. In *Conference on Robot Learning*, 2019.
- Peng, X. B., Kumar, A., Zhang, G., and Levine, S. Advantage-Weighted Regression: Simple and scalable off-policy reinforcement learning. *arXiv preprint arXiv:1910.00177*, 2019.
- Peters, J. and Schaal, S. Reinforcement learning by reward-weighted regression for operational space control. In *Proceedings of the 24th international conference on Machine learning*, 2007.
- Peters, J., Mülling, K., and Altün, Y. Relative entropy policy search. In *AAAI Conference on Artificial Intelligence*, 2010.
- Rawlik, K., Toussaint, M., and Vijayakumar, S. On stochastic optimal control and reinforcement learning by approximate inference. In *International Joint Conference on Artificial Intelligence*, 2012.
- Schulman, J., Levine, S., Moritz, P., Jordan, M., and Abbeel, P. Trust region policy optimization. In *International Conference on Machine Learning*, 2015.
- Schulman, J., Moritz, P., Levine, S., Jordan, M., and Abbeel, P. High-dimensional continuous control using generalized advantage estimation. In *International Conference on Learning Representations*, 2016.
- Schulman, J., Wolski, F., Dhariwal, P., Radford, A., and Klimov, O. Proximal policy optimization algorithms. *arXiv preprint arXiv:1707.06347*, 2017.
- Siegel, N. Y., Springenberg, J. T., Berkenkamp, F., Abdolmaleki, A., Neunert, M., Lampe, T., Hafner, R., and Riedmiller, M. A. Keep doing what worked: Behavioral modelling priors for offline reinforcement learning. In *International Conference on Learning Representations*, 2020.
- Song, H. F., Abdolmaleki, A., Springenberg, J. T., Clark, A., Soyer, H., Rae, J. W., Noury, S., Ahuja, A., Liu, S., Tirumala, D., Heess, N., Belov, D., Riedmiller, M., and Botvinick, M. M. V-mpo: On-policy maximum a posteriori policy optimization for discrete and continuous control. In *International Conference on Learning Representations*, 2020.
- Tang, Y. and Kucukelbir, A. Hindsight expectation maximization for goal-conditioned reinforcement learning. *arXiv preprint arXiv:2006.07549*, 2020.
- Tassa, Y., Doron, Y., Muldal, A., Erez, T., Li, Y., de Las Casas, D., Budden, D., Abdolmaleki, A., Merel, J., Lefrancq, A., Lillicrap, T., and Riedmiller, M. Deepmind control suite. *arXiv preprint arXiv:1801.00690*, 2018.
- Todorov, E. General duality between optimal control and estimation. In *IEEE Conference on Decision and Control*, 2008.
- Todorov, E. et al. Linearly-solvable markov decision problems. In *Advances in Neural Information Processing Systems*, 2006.
- Toussaint, M. Robot trajectory optimization using approximate inference. In *International Conference on Machine Learning*, 2009.
- Toussaint, M. and Storkey, A. Probabilistic inference for solving discrete and continuous state markov decision processes. In *International conference on Machine learning*, 2006.
- Tucker, G., Bhupatiraju, S., Gu, S., Turner, R., Ghahramani, Z., and Levine, S. The mirage of action-dependent baselines in reinforcement learning. In *International Conference on Machine Learning*, 2018.
- Vieillard, N., Kozuno, T., Scherrer, B., Pietquin, O., Munos, R., and Geist, M. Leverage the average: an analysis of kl regularization in rl. In *Advances in Neural Information Processing Systems*, 2021.
- Wang, T., Bao, X., Clavera, I., Hoang, J., Wen, Y., Langlois, E., Zhang, S., Zhang, G., Abbeel, P., and Ba, J. Benchmarking model-based reinforcement learning. *arXiv preprint arXiv:1907.02057*, 2019.
- Wang, Z., Novikov, A., Zolna, K., Springenberg, J. T., Reed, S., Shahriari, B., Siegel, N., Merel, J., Gulcehre, C., Heess, N., and de Freitas, N. Critic regularized regression. *arXiv preprint arXiv:2006.15134*, 2020.
- Wu, C., Rajeswaran, A., Duan, Y., Kumar, V., Bayen, A. M., Kakade, S., Mordatch, I., and Abbeel, P. Variance reduction for policy gradient with action-dependent factorized baselines. *arXiv preprint arXiv:1803.07246*, 2018.

Wu, Y., Tucker, G., and Nachum, O. Behavior Regularized Offline Reinforcement Learning. *arXiv preprint arXiv:1911.11361*, 2019.

## Appendix

### A. Network Architectures

Architecture	MPO	AWR	SAC
Policy network	(256, 256, 256)	(128, 64)	(256, 256)
Value network	(512, 512, 256)	(128, 64)	(256, 256)
Activation function	ELU	ReLU	ReLU
Layer normalization	✓	–	–
Input normalization	–	✓	–
Optimizer	Adam	SGD (momentum=0.9)	Adam
Learning rate (policy)	1e-4	5e-5	3e-4
Learning rate (value)	1e-4	1e-2	3e-4
Weight initialization	Uniform	Xavier Uniform	Xavier Uniform
Initial output scale (policy)	1.0	1e-4	1e-2

Table 4. Details of each network architecture. We refer the original implementations of each algorithm which is available online (Haarnoja et al., 2018b; Fujita et al., 2019; Peng et al., 2019; Hoffman et al., 2020). Note that AWR uses different learning rates of the policy per environment.

### B. Benchmarks on MuJoCo Manipulation Tasks

We extensively evaluate their performance in the manipulation tasks (Figure 4). The trend seems the same as the locomotion tasks, while AWR beats SAC and MPO in Striker, which means they fall into sub-optimal.

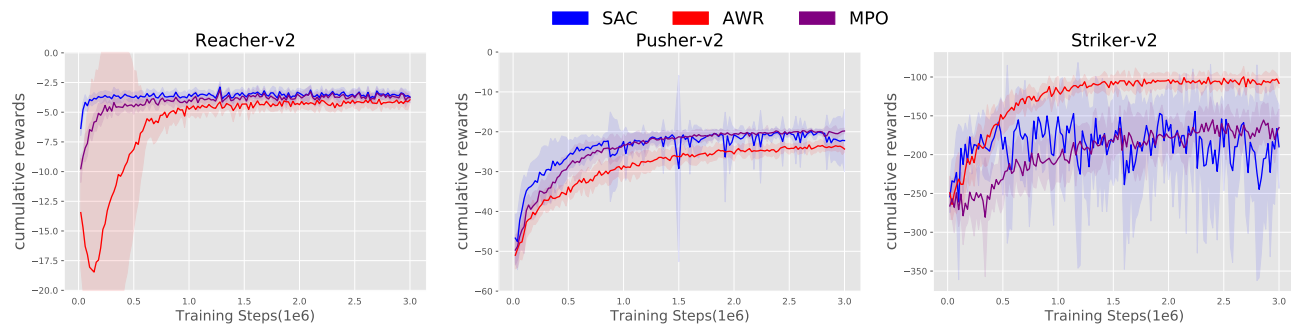


Figure 4. Benchmarking results on OpenAI Gym MuJoCo manipulation environments. All experiments are run with 10 random seeds. SAC and MPO completely solve Reacher and Pusher, while in Striker they fall into sub-optimal.

We mainly used 4 GPUs (NVIDIA V100; 16GB) for the experiments in Section 4.3 and 5 and it took about 4 hours per seed (3M steps).

## C. Relations to Other Algorithms

We here explain the relation of the unified policy iteration scheme covers other algorithms. While we mainly focused on AWR, MPO, and SAC in the this paper, our unified scheme covers other algorithms too, as summarized in [Table 1](#):

### EM control algorithms:

- **POWER (Kober & Peters, 2008)**:  $\pi_p (= \pi_\theta)$  update is analytic.  $\mathcal{G} = \eta \log Q^{\pi_p}$  and  $Q^{\pi_p}$  is estimated by TD(1).  $\pi_\theta = \mathcal{N}(\mu_\theta(s), \Sigma_\theta(s))$ .
- **RWR (Peters & Schaal, 2007)**:  $\pi_p = \pi_\theta$  is updated by SG.  $\mathcal{G} = \eta \log r$ , and  $\pi_\theta = \mathcal{N}(\mu_\theta(s), \Sigma)$ . When the reward is unbounded, RWR requires adaptive reward transformation (e.g.  $u_\beta(r(s, a)) = \beta \exp(-\beta r(s, a))$ ;  $\beta$  is a learnable parameter).
- **REPS (Peters et al., 2010)**:  $\pi_p$  is  $\pi_q$  of the previous EM step (on-policy) or a mixture of all previous  $\pi_q$  (off-policy), which is approximated by samples.  $\mathcal{G} = A^{\pi_p}$  and estimated by a single-step TD error with a state-value function computed by solving a dual function.  $\pi_q$  is assumed as a softmax policy for discrete control in the original paper.
- **UREX (Nachum et al., 2017)**:  $\pi_p = \pi_\theta$  is updated by SG.  $\mathcal{G} = Q^{\pi_p}$  and estimated by TD(1).  $\pi_\theta$  is assumed as a softmax policy for discrete control in the original paper.
- **V-MPO (Song et al., 2020)**: Almost the same as MPO, but a state-value function is trained by  $n$ -step bootstrap instead of Q-function. Top-K advantages are used in E-step.

### KL control algorithms:

- **TRPO (Schulman et al., 2015)**:  $\pi_q = \pi_\theta = \mathcal{N}(\mu_\theta(s), \Sigma_\theta)$ . The KL penalty is converted to a constraint, and the direction of the KL is reversed.  $\mathcal{G} = A^{\pi_p}$  and estimated by TD(1).  $\pi_p$  is continuously updated to  $\pi_q$ .
- **PPO with a KL penalty (Schulman et al., 2017)**:  $\pi_q = \pi_\theta = \mathcal{N}(\mu_\theta(s), \Sigma_\theta)$ . The direction of the KL penalty is reversed.  $\mathcal{G} = A^{\pi_p}$  and estimated by GAE (Schulman et al., 2016). An adaptive  $\eta$  is used so that  $D_{KL}(\pi_p || \pi_q)$  approximately matches to a target value.
- **DDPG<sup>2</sup> (Lillicrap et al., 2016)**:  $\pi_q = \pi_\theta$  is the delta distribution and updated by SG.  $\mathcal{G} = Q^{\pi_q}$  and estimated by TD(0).  $\eta = 0$  (i.e., the KL divergence and  $\pi_p$  update are ignored).
- **TD3<sup>2</sup> (Fujimoto et al., 2018)**: It is a variant of DDPG and leverages three implementational techniques, clipped double Q-learning, delayed policy updates, and target policy smoothing.
- **BRAC (Wu et al., 2019) and BEAR (Kumar et al., 2019) (Offline RL)**: When we assume  $\pi_p = \pi_b$  (any behavior policy), and omitting its update, some of the offline RL methods, such as BRAC or BEAR, can be interpreted as one of the KL control methods. Both algorithms utilize the variants of clipped double Q-learning ( $\lambda$ -interpolation between max and min).

<sup>2</sup>Note that DDPG and TD3 are not the “inference-based” algorithms, but we can classify these two as KL control variants.

## D. Reproduction Results of AWR on MuJoCo Locomotion Environments

We re-implemented AWR based on PFRL, a PyTorch-based RL library (Fujita et al., 2019), referring its original implementation (Peng et al., 2019). Figure 5 shows the performance of our implementation in the original experimental settings, also following hyper-parameters. We recovered the original results in Peng et al. (2019) properly.

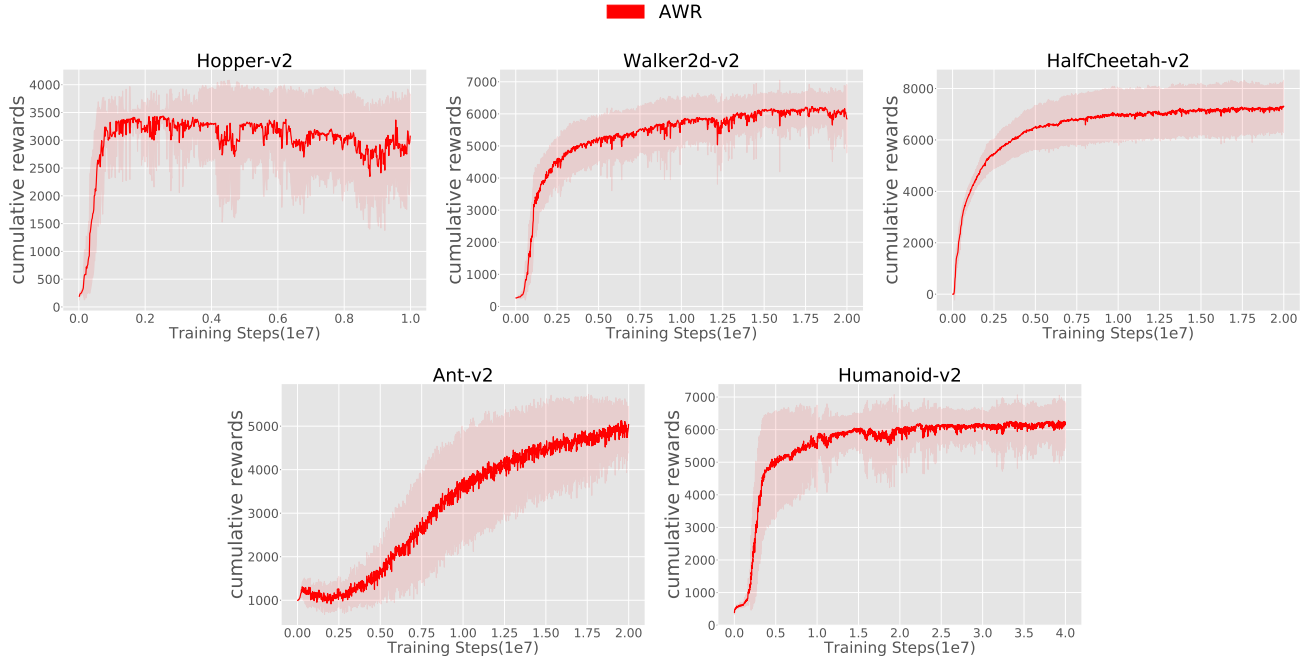


Figure 5. Reproduction of Advantage Weighted Regression (AWR). We obtained comparable results to the original paper.

## E. Performances of Each Algorithms in Section 5.3

We present results of ablation study in Section 5.3. These results suggest that these off-policy inference-based algorithms might be fragile with other network architectures and more co-dependent with architectures than on-policy algorithms.

Algorithm	Architecture		
	MPO	AWR	SAC
MPO	2136 $\pm$ 1047	623 $\pm$ 316	1108 $\pm$ 828
AWR	2509 $\pm$ 1117	<b>3085 <math>\pm</math> 593</b>	2352 $\pm$ 960
SAC	2239 $\pm$ 669	651 $\pm$ 381 <sup>†</sup>	3013 $\pm$ 602

Table 5. Results in Hopper-v2 environment (<sup>†</sup>numerical error happens during training). All results are averaged over 10 seeds and we also show their standard deviations.

Algorithm	Architecture		
	MPO	AWR	SAC
MPO	3972 $\pm$ 849	481 $\pm$ 210	1548 $\pm$ 1390
AWR	1312 $\pm$ 680 <sup>†</sup>	4717 $\pm$ 678	428 $\pm$ 89
SAC	5598 $\pm$ 795	117 $\pm$ 164	<b>5820 <math>\pm</math> 556</b>

Table 6. Results in Walker2d-v2 environment (<sup>†</sup>numerical error happens during training). All results are averaged over 10 seeds and we also show their standard deviations.

Algorithm	Architecture		
	MPO	AWR	SAC
MPO	11769 ± 321	339 ± 517	−∞
AWR	485 ± 57	5742 ± 667	1060 ± 146
SAC	<b>16541 ± 341</b>	589 ± 367 <sup>†</sup>	15254 ± 751

Table 7. Results in HalfCheetah-v2 environment (<sup>†</sup>numerical error happens during training). All results are averaged over 10 seeds and we also show their standard deviations.

Algorithm	Architecture		
	MPO	AWR	SAC
MPO	6584 ± 455	967 ± 202	−∞
AWR	−30 ± 12	1127 ± 224	243 ± 167
SAC	<b>7159 ± 1577</b>	479 ± 463 <sup>†</sup>	5532 ± 1266

Table 8. Results in Ant-v2 environment (<sup>†</sup>numerical error happens during training). All results are averaged over 10 seeds and we also show their standard deviations.

Algorithm	Architecture		
	MPO	AWR	SAC
MPO	5709 ± 1081	288 ± 126	371 ± 72
AWR	420 ± 30	5573 ± 1020	507 ± 48
SAC	<b>9225 ± 1010</b>	205 ± 0	8081 ± 1149

Table 9. Results in Humanoid-v2 environment. All results are averaged over 10 seeds and we also show their standard deviations.

Algorithm	Architecture		
	MPO	AWR	SAC
MPO	70 ± 40	41 ± 15	−∞
AWR	124 ± 3	128 ± 4	<b>130 ± 8</b>
SAC	53 ± 6 <sup>†</sup>	47 ± 3	114 ± 21

Table 10. Results in Swimmer-v2 environment (<sup>†</sup>numerical error happens during training). All results are averaged over 10 seeds and we also show their standard deviations.

## F. Full results

In this section, we present full results (Figures and Table) in Section 5.

### F.1. Clipped Double Q-Learning

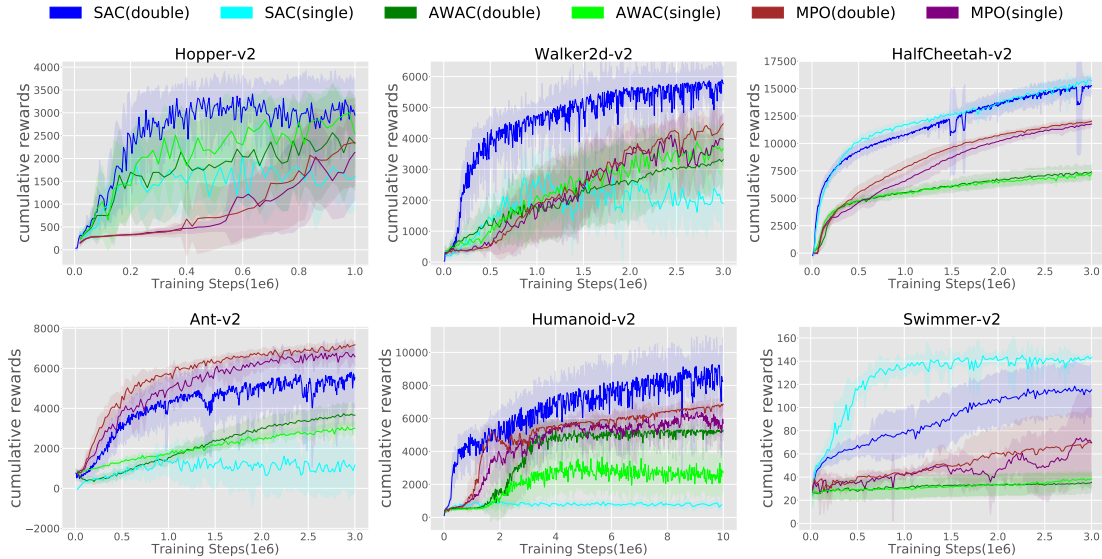


Figure 6. Ablation of Clipped Double Q-Learning (Fujimoto et al., 2018). We test original SAC (double), AWAC (double), MPO (single), and some variants; SAC without clipped double Q-learning (single), AWAC (single), and MPO with clipped double Q-learning (double). SAC without clipped double Q-learning beats the original one in HalfCheetah and Swimmer, while fails to learn in Hopper, Walker, Ant, and Humanoid, which implies that single-Q SAC becomes a highly exploratory policy, since it fails in environments with termination.

### F.2. The distribution of the policy

The learning curves are shown in Figure 7.

### F.3. Effect on ELU and Layer Normalization

We here present the detailed results of Section 5.4. To obtain much deeper observation on the effect of some code-level regularization techniques in MPO, we combine ELU activation (Clevert et al., 2016) and layer normalization (Ba et al., 2016) into SAC, while keeping the original implementation of SAC in the other components.

Figure 8 shows that layer normalization and ELU mostly contribute to the highest performance of SAC in Ant and Swimmer, where MPO and AWR archives the best in Figure 1 before. While we could not see such significant gains in the other environments (slight improvement with ELU in HalfCheetah; no changes in Walker2d and Humanoid; degradation in Hopper), properly architecture-tuned SAC performs the mostly-best in all environments. Note that MPO removing these code-level implementation details (orange) largely decreases the performances. This observation suggests that the implementation of MPO might be highly co-adapted to some code-level regularization techniques, but transferable and highly beneficial to KL control methods. To ensure the coverage of environments, we test incorporating ELU and layer normalization to SAC in 12 DM Control tasks. See Appendix G for the details.

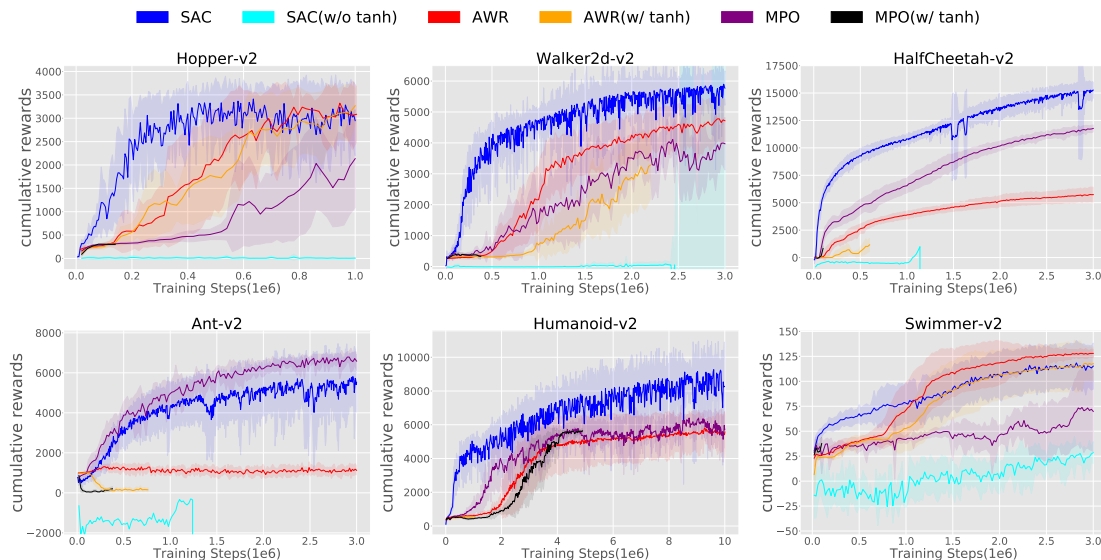


Figure 7. Ablation of Tanh transformation. We test SAC without tanh-squashed distribution, AWR with tanh, and MPO with tanh. SAC without tanh transform (using MPO action penalty instead) results in drastic degradation of the performance, which can be caused by the maximum entropy objective that encourages the maximization of the covariance. AWR and MPO with tanh squashing become numerically unstable. A line that stopped in the middle means that its training has stopped at that step due to numerical error.

	SAC	SAC-E <sup>+</sup>	SAC-L <sup>+</sup>	SAC-E <sup>+</sup> L <sup>+</sup>	MPO	MPO-E <sup>-</sup> L <sup>-</sup>	AWR
Hopper-v2	<b>3013 ± 602</b>	2337 ± 903	2368 ± 179	1926 ± 417	2136 ± 1047	843 ± 168	<b>3085 ± 593</b>
Walker2d-v2	<b>5820 ± 411</b>	5504 ± 431	5613 ± 762	5751 ± 400	3972 ± 849	1708 ± 663	4717 ± 678
HalfCheetah-v2	15254 ± 751	<b>15350 ± 594</b>	13074 ± 2218	12555 ± 1259	11769 ± 321	-1363 ± 20965	5742 ± 667
Ant-v2	5532 ± 1266	6457 ± 828	<b>7349 ± 176</b>	7017 ± 132	6584 ± 455	807 ± 2351	1127 ± 224
Humanoid-v2	8081 ± 1149	<b>8196 ± 892</b>	8146 ± 470	7687 ± 1385	5709 ± 1081	5566 ± 787	5573 ± 1020
Swimmer-v2	114 ± 21	<b>146 ± 7</b>	99 ± 18	143 ± 9	70 ± 40	-∞	128 ± 4

Table 11. Raw scores of Figure 8. SAC with ELU (-E<sup>+</sup>) or layer normalization (-L<sup>+</sup>) achieves the best performances in several tasks.

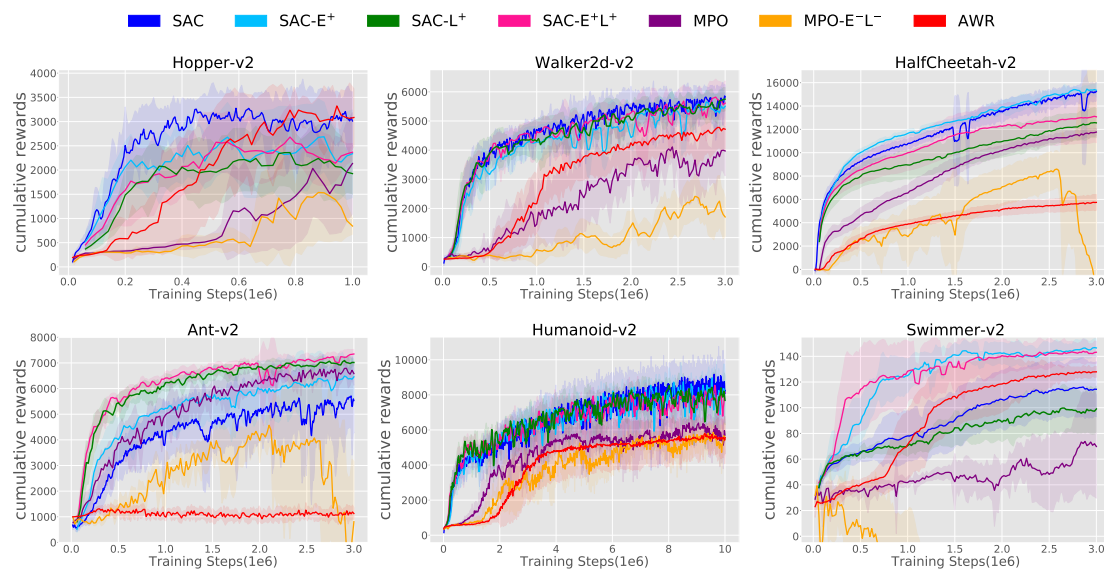


Figure 8. Comparison between original SAC and combination of implementation details in MPO, ELU and layer normalization. E<sup>+</sup>/L<sup>+</sup> indicates adding, and E<sup>-</sup>/L<sup>-</sup> indicates removing ELU/layer normalization. Introducing layer normalization or ELU into original SAC (light blue, green, pink) improves the performances in Ant (beating MPO), Swimmer (beating AWR), HalfCheetah, and Humanoid.

## G. Benchmarks on DeepMind Control Suite

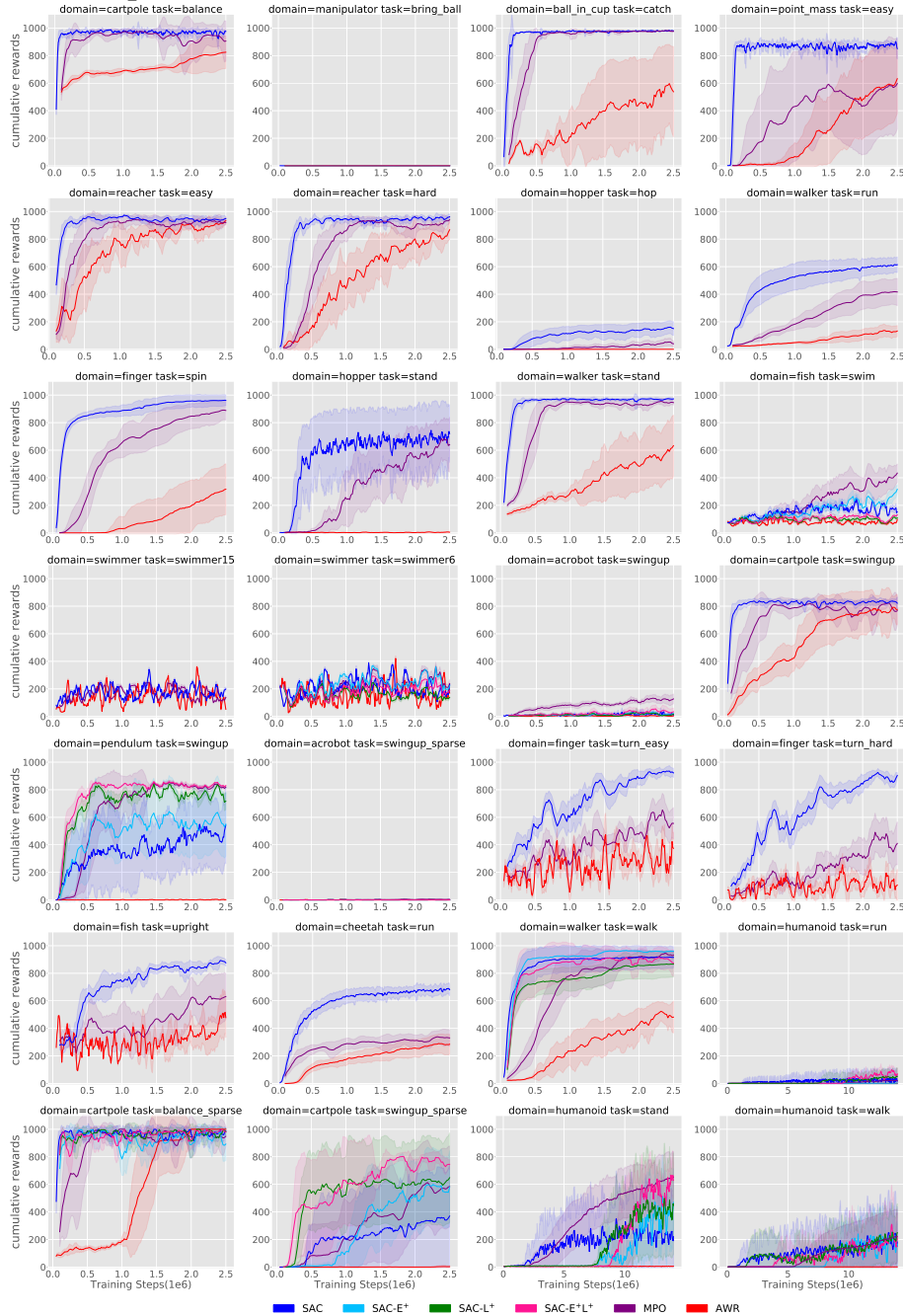


Figure 9. Benchmarking results on DeepMind Control Suite 28 environments. The performances are averaged among 10 random seeds.

In this section, we show the benchmarking results on 28 tasks in DeepMind Control Suite (Figure 9). Each algorithm is run with 2.5M steps (except for humanoid domain; 14M steps), following Abdolmaleki et al. (2018b). While the previous work mentioned that tuning the number of action repeats was effective (Lee et al., 2020), we used an action repeat of 1 throughout all experiments for simplicity. We also use the hyper-parameters of each algorithm presented in Appendix A. As discussed in Section 5.4, we incorporate ELU and layer normalization into SAC in several domains where SAC is behind MPO or AWR. ELU and layer normalization significantly improve performances, especially in pendulum\_swingup and cartpole\_swingup\_sparse. Some of MPO results don't seem to match the original paper, but we appropriately confirmed that these results are equivalent to those of its public implementation (Hoffman et al., 2020).

	SAC	SAC-E <sup>+</sup>	SAC-L <sup>+</sup>	SAC-E <sup>+</sup> L <sup>+</sup>	MPO	AWR
cartpole_balance	<b>975 ± 12</b>	–	–	–	824 ± 118	905 ± 146
manipulator_bring_ball	0.27 ± 0.0	0.80 ± 0.1	<b>0.96 ± 0.3</b>	0.72 ± 0.1	0.79 ± 0.1	0.85 ± 0.2
ball_in_cup_catch	<b>980 ± 0.5</b>	–	–	–	976 ± 6	538 ± 328
point_mass_easy	<b>850 ± 75</b>	–	–	–	632 ± 254	597 ± 329
reacher_easy	<b>949 ± 14</b>	–	–	–	920 ± 18	934 ± 25
reacher_hard	<b>962 ± 18</b>	–	–	–	941 ± 22	868 ± 70
hopper_hop	<b>151 ± 50</b>	–	–	–	41 ± 22	0.1 ± 0.2
walker_run	<b>615 ± 56</b>	–	–	–	416 ± 99	133 ± 40
finger_spin	<b>962 ± 39</b>	–	–	–	888 ± 69	317 ± 185
hopper_stand	<b>720 ± 207</b>	–	–	–	640 ± 199	5 ± 1
walker_stand	<b>972 ± 6</b>	–	–	–	945 ± 18	633 ± 221
fish_swim	152 ± 23	317 ± 32	108 ± 9	130 ± 6	<b>434 ± 66</b>	97 ± 13
swimmer_swimmer15	<b>199 ± 15</b>	–	–	–	139 ± 14	52 ± 4
swimmer_swimmer6	229 ± 12	223 ± 11	138 ± 13	189 ± 17	<b>238 ± 29</b>	170 ± 4
acrobot_swingup	10 ± 10	21 ± 10	15 ± 7	34 ± 27	<b>127 ± 36</b>	4 ± 2
cartpole_swingup	<b>822 ± 45</b>	–	–	–	776 ± 109	767 ± 106
pendulum_swingup	542 ± 279	550 ± 232	718 ± 62	<b>830 ± 4</b>	819 ± 11	1 ± 4
acrobot_swingup_sparse	0.40 ± 0.1	0.43 ± 0.2	0.46 ± 0.0	0.42 ± 0.1	<b>4 ± 4</b>	0.0 ± 0.0
finger_turn_easy	<b>922 ± 34</b>	–	–	–	556 ± 116	374 ± 117
finger_turn_hard	<b>904 ± 21</b>	–	–	–	410 ± 156	109 ± 113
fish_upright	<b>876 ± 25</b>	–	–	–	631 ± 166	478 ± 143
cheetah_run	<b>682 ± 44</b>	–	–	–	331 ± 60	285 ± 73
walker_walk	916 ± 77	<b>960 ± 7</b>	866 ± 93	875 ± 97	931 ± 25	482 ± 115
humanoid_run	17 ± 47	3 ± 2	52 ± 62	<b>71 ± 39</b>	22 ± 42	0.8 ± 0.0
cartpole_balance_sparse	987 ± 27	892 ± 119	982 ± 30	982 ± 10	949 ± 76	<b>1000 ± 0.0</b>
cartpole_swingup_sparse	370 ± 370	582 ± 261	648 ± 324	<b>745 ± 36</b>	585 ± 294	3 ± 10
humanoid_stand	221 ± 231	469 ± 245	448 ± 359	630 ± 129	<b>651 ± 183</b>	6 ± 0.0
humanoid_walk	182 ± 255	166 ± 148	<b>250 ± 209</b>	219 ± 177	224 ± 197	1 ± 0.0

Table 12. Raw scores of Figure 9. The performances are averaged among 10 random seeds. Each algorithm is run with 2.5M steps (except for humanoid domain; 14M steps), following Abdolmaleki et al. (2018b). We use an action repeat of 1 throughout all experiments for simplicity.